

IAC-10-A6.1.07

**PHYSICAL CHARACTERIZATION OF HIGH AMR DEBRIS BY
OPTICAL REFLECTANCE SPECTROMETRY**

T. Schildknecht

Astronomical Institute, University of Bern, CH-3012 Bern, Switzerland
thomas.schildknecht@aiub.unibe.ch

A. Vananti¹, H. Krag², C. Erd³

²Astronomical Institute, University of Bern, CH-3012 Bern, Switzerland

²ESA ESOC, Robert-Bosch-Strasse 5, 64293 Darmstadt, Germany

³ESA ESTEC, Keplerlaan 1, 2200 AG Noordwijk, The Netherlands

ABSTRACT

One of the primary objectives in the characterization of the space debris environment is the identification of the physical properties of the space debris objects. Reflectance spectroscopy is a very promising technique to remotely investigate the surface material of these objects. First spectroscopic observations of debris objects in GEO were acquired during several campaigns in 2009. The results from these campaigns were very promising and encouraged the continuation of these observations in 2010. The measurements were conducted at the 1-meter ESA Space Debris Telescope (ESASDT) on Tenerife with a low-resolution spectrograph in the wavelength range of 450-960 nm. In this work a compilation of the measurements of the campaigns 2009 and 2010 is presented. With respect to the first results additional objects in GEO, GTO and fragments with high area-to-mass ratios were observed. Furthermore an improved accuracy in the reduction of the spectroscopy data has been achieved.

Samples of satellite surface materials employed by the space industry were measured with a spectrometer in the laboratory and the obtained spectra compared with remote measurements of space objects. Using these laboratory references a preliminary attempt to classify different types of spectra was made.

INTRODUCTION

The characterization of the space debris environment at high altitudes mostly involves optical observations by means of ground-based optical telescopes. The debris surveys include the discovery of new objects, the determination and maintenance of their orbits, and possibly the investigation of the physical properties of these objects. Optical surveys provide astrometric positions and the brightness (magnitude) of the objects. The positions are used to determine and maintain the orbits of the objects and thereby to determine the area-to-mass ratio (AMR). Magnitudes and their variations may be used to estimate object sizes and attitude changes. The conversion of the magnitudes to physical sizes, however, requires detailed knowledge of the surface properties and the shapes of the objects (albedo, amount of specular vs. diffuse reflection, color, etc.). Sequences of brightness measurements over time, so-called light curves, may give some indication about the objects shapes and the tumbling or rotation rates. Measurements of some GEO debris objects with the ZIMLAT telescope showed a wide variety of temporal variations with time scales ranging from a fraction of a second to tens of minutes [1][2]. Other teams reported color photometry observations of objects in GEO-like orbits [1][3]. Such observations could provide information on the surface material of the objects, however, the determination of colors proved to be difficult due to strong temporal brightness changes of the objects (the observation systems used in these studies could not measure multiple colors in parallel). Consequently the current results are not conclusive.

Reflection spectra obtained with a spectrograph, on the other hand, provide a simultaneous measurement of the brightness of the object over a wide wavelength range. Reflection spectra of rocket bodies in LEO and GEO were reported by a NASA team already in 2001 [4]. In the same paper the authors perform a first comparison of these spectra with spectra of material samples taken in the laboratory.

The aim of this work was to obtain the first reflection spectra of small-size debris objects in high-altitude orbits. Of particular interest was the investigation of the high AMR objects in GEO-like orbits. A common hypothesis is that these objects could be pieces of lightweight surface materials of spacecraft and rocket bodies like solar cells or parts of multi-layer insulation blankets. Comparing remotely ob-

served reflection spectra of high AMR objects with spectra of spacecraft materials obtained in the laboratory is a promising technique to eventually determine the nature and origin of the high AMR population.

This paper presents results from the experimental observation campaigns conducted with the 1-meter ESA Space Debris Telescope (ESASDT) on Tenerife during the years 2009 and 2010.

EXPERIMENTAL SETUP

The spectroscopic observations were performed with a low-resolution spectrograph mounted at RC-focus of the 1-meter ESASDT telescope. The spectrograph was originally designed for observations of comets and is clearly not optimized for observing space debris. The dispersive element of this spectrograph is a transmission grating, more precisely a combination of a grating with a prism, a so-called 'grism' (the prism is used to bring the desired wavelength range (order) back to the optical axis). Three different grisms with 150, 478, and 222 lines/mm, respectively, are available. The resulting spectrum is detected by a liquid nitrogen cooled 2k x 2k CCD camera. The selection of the grism was entirely dictated by signal-to-noise considerations. The target objects were all expected to be fainter than magnitude 12, most of the high AMR objects are even in the range of magnitude 16 to 17. When observing spectra of stars or solar system objects these magnitudes would not pose any particular difficulty but merely require long exposure times of the order of several ten minutes. The maximum observation time for moving objects is much shorter and is primarily given by the density of the stellar background (at magnitudes equal or brighter than the target object): every once in a while the object 'crosses' a star, which will contaminate the measurement. Given these restrictions we decided to maximize the signal-to-noise ratio per pixel by using the grism with the lowest dispersion. This grism has a center wavelength of 510 nm and provides a resolution of 0.4 nm per pixel over a wavelength range from 450 to 960 nm.

OBSERVATIONS AND DATA REDUCTION

The observations took place during 6 nights in November 08, 5 in January 09, 3 in May 09, and 7 in

June 2010. Eventually only two thirds of the nights were of sufficient atmospheric quality, so-called ‘photometric’ nights.

Due to the experimental character of the observations we selected rather bright GEO objects with well known orbits as our first targets. We then gradually moved to fainter objects and finally observed a series of high AMR objects which were fainter than magnitude 16.

The aim of reflectance spectroscopy is always a quantitative comparison of the measured spectrum with the spectrum of the illuminating source, in our case, the Sun. The calibration of the science observations should therefore ideally be done by measuring the Sun. During nighttime so-called ‘solar analog’ stars are observed, whose spectra resemble the solar spectrum to great extent. These stars are then used as calibration sources instead of the Sun.

Standard data reduction procedures were applied to obtain wavelength-calibrated spectra. The reduction task includes the elimination of cosmic ray events from the raw frames, the subtraction of the sky background, binning of the two-dimensional spectra into one-dimensional ‘scans’ and finally calibration of the dispersion using the calibration lamp exposures. After these steps, the series of multiple observations of the same object (or calibration star) taken within a short time interval were stacked together.

At this stage the spectra are still affected by the wavelength-dependent atmospheric extinction and the wavelength-dependent response function of the spectrograph.

Two different approaches were adopted for the extinction correction of the OGS spectra: individual extinction curves for each night derived from the observations themselves, or correction using mean extinction curve. In order to derive the extinction curve for a single night spectra of solar analog stars measured at different air mass values were used. Figure 1 shows four spectra of a solar analog star at different air masses illustrating the strong effect of atmospheric extinction on the overall shape of the observed spectra. The spectra were normalized to unity at an arbitrary value of 550 nm. Alternatively, if the solar analog stars were observed over an insufficient range of air masses, a mean extinction curve was used. Figure 2 shows the mean extinction curve for the La Silla Observatory (ESO, Chile). Although mean extinction curves do not reflect the actual extinction of the night, representing usually

e.g. the monthly averaged extinction or the extinction during certain periods of the year, the errors with respect to the true extinction are still acceptable.

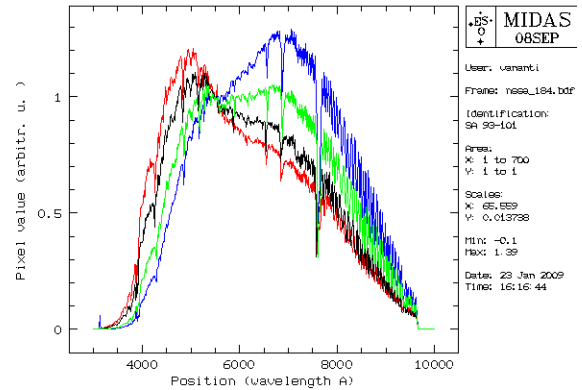


Figure 1: Normalized spectra of solar analog stars at different air mass. The red, black green and blue curves are spectra obtained at 1.01, 1.13, 1.4 and 1.94 air mass, respectively.

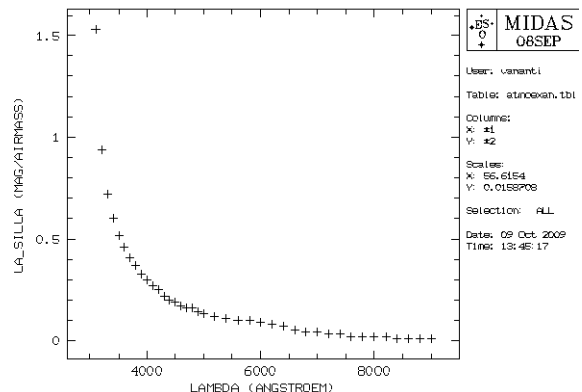


Figure 2: Mean extinction curve for the La Silla Observatory (ESO, Chile).

The wavelength-dependent response function of the spectrograph needs not to be determined explicitly when performing relative reflectance spectroscopy. The reflectance of the program object is obtained by dividing the extinction-corrected spectrum of the object by the extinction-corrected spectrum of a solar analogue star. As the spectra of the program object and the solar analogue star are both affected by the same response function, the latter cancels.

RESULTS

Spectra of geostationary satellites

The spectra of active GEO satellites with known materials have been measured to investigate the possibility of remotely identifying spacecraft surface materials from spectral data. Furthermore, satellites represent relatively easy targets to start with, since they are comparably bright (brighter than 15 mag) and their orbits are well known. For the investigations the following satellites were chosen: Artemis (Cospar ID 01029A), Astra 1D (94070A), Meteosat MSG-1 (05049B), and MSG-2 (02040B). Figure 3 displays one measured spectrum of MSG-1. The additional red curve is an interpolation of selected points of the spectrum. This representation will be used in the following to compare different spectra, especially in those cases where the spectral signal is very disturbed by noise and fringes. MSG satellites are spin-stabilized satellites (about 100 rotations per minute) with the rotation axis almost parallel to the Earth's axis. The cylindrical surface is mostly covered by solar cells.

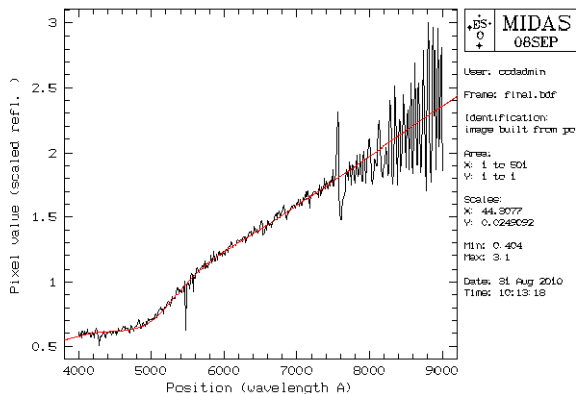


Figure 3: Spectrum of Meteosat satellite MSG-1 (05049B).

In Figure 4 spectra of MSG-1 measured with phase angles of 53°, 27°, and 60° are plotted. The spectra do not exhibit a clear angle dependence, as expected from geometric considerations. The slight differences between the spectra lie within a probable error range.

Contrary to MSG satellites, Artemis and Astra 1D are three-axis stabilized satellites. In theory, since their solar panels are always oriented towards the Sun, there should be a phase angle dependence. Figure 5 shows measurements of Artemis at 17° and

52° phase angle, respectively. There is no obvious difference of the spectra for the two phase angles, on the contrary, the curves coincide extremely well up to 800 nm.

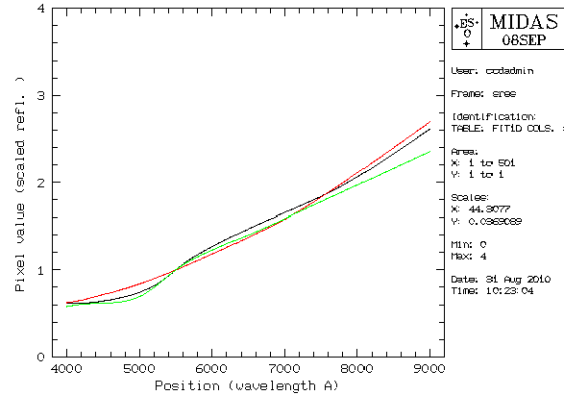


Figure 4: Spectra of MSG-1 measured at different phase angles: 53° (black), 27° (red), 60° (green).

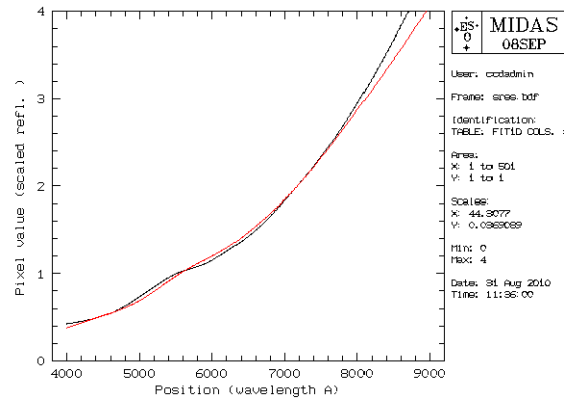


Figure 5: Spectra of satellite Artemis at different phase angles: 17° (black), 52° (red).

Spectra of space debris

The spectra of the debris objects show several characteristics, slope variations, and different shapes. These 'features' may possibly be used to classify debris fragments and ultimately to determine the type of surface material. Figure 6 shows the spectra of the bright (mag=13.4±1.2), low AMR (AMR=0.02 m²/kg) GTO debris object S92005 taken on different nights. The spectra exhibit big similarities and an almost identical slope between 500 nm and 900 nm. Obviously the reproducibility can be guaranteed only under the condition that the phase angle remains approximately constant and the object did not rotate or change its orientation between the measurements, or the object's shape and

material composition is such that the resulting reflection spectrum is independent of its attitude and phase angle. Like the object S92005, most of the measured objects show an increasing of the reflectance with increasing wavelength in the region between 600 nm and 900 nm. This increase of the reflectance at longer wavelengths might be due to the so-called ‘reddening’ of material surfaces in space. Remotely observed spectra of certain objects with known surface materials proved to be essentially darker and redder than their analog laboratory spectra [5]. The ‘reddening effect’ is probably caused by space weathering. Modeling the extent of the reddening seems to be rather difficult [6].

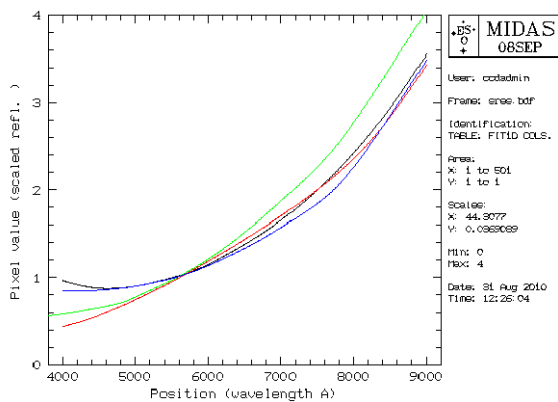


Figure 6: Spectra of the bright GTO debris object S92005 taken on different nights ($\text{mag}=13.4\pm 1.2$, $\text{AMR}=0.02 \text{ m}^2/\text{kg}$).

Some of the measured objects exhibit different spectra depending on the measurement epoch. Figure 7 illustrates the variation of spectra of the bright ($\text{mag}=12.8\pm 1.3$), low AMR ($\text{AMR}=0.04 \text{ m}^2/\text{kg}$), GEO debris objects E08152A taken on different nights. The difference is pronounced and it is not within a reasonable error range. Most likely two different faces of the same rotating or tumbling object were measured. Additional measurements of object E08211A from other nights show spectra resembling one or the other spectrum of Figure 7.

The spectra of the bright ($13.1\pm 1.0 \text{ mag}$), low AMR ($0.02 \text{ m}^2/\text{kg}$), ‘eccentric GEO’ debris E08152A given in Figure 8 show significantly different characteristics. The spectra are ‘convex’ and the reflectance decreases with increasing wavelength. In the region between 600 nm and 800 nm the spectra become relatively flat.

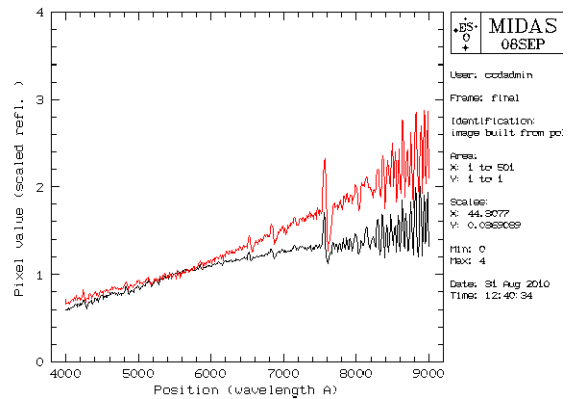


Figure 7: Spectra of the bright ($\text{mag}=12.8\pm 1.3$), low AMR ($\text{AMR}=0.04 \text{ m}^2/\text{kg}$), GEO debris object E08211A taken on different nights.

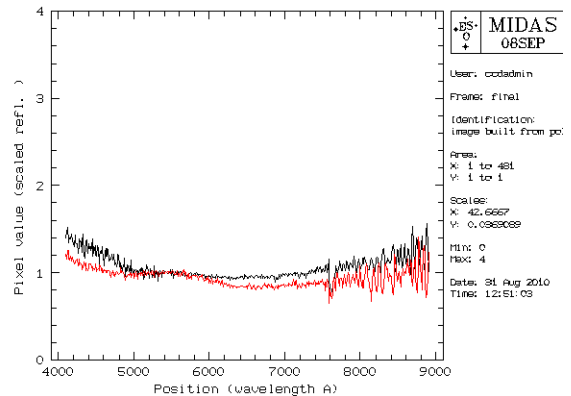


Figure 8: Spectra of the bright ($13.1\pm 1.0 \text{ mag}$), low AMR ($0.02 \text{ m}^2/\text{kg}$), ‘eccentric GEO’ debris object E08152A measured on different nights.

Eventually spectra of some faint, high AMR objects were taken. Examples are given Figure 9, Figure 10, and Figure 11. The faint ($\sim 16 \text{ mag}$), high AMR ($0.5 \text{ m}^2/\text{kg}$), ‘eccentric GEO’ debris E07046Bn (Figure 9) shows distinct spectra at different epochs, which is an indication that the object may consist of a mix of different surface materials (e.g. a front and a back side). The spectra of the high AMR ($3.0 \text{ m}^2/\text{kg}$), ‘eccentric GEO’ debris object N2010067 (Figure 10) exhibit a distinct sharp bend around 500 nm and then strongly increasing reflectivity for longer wavelengths (with ‘concave’ shape). Distinct features like this ‘knee’ should hopefully allow identifying materials.

Finally, spectra of a debris object with an extremely high AMR of $29.3 \text{ m}^2/\text{kg}$ are given in Figure 11. The spectra from two nights are very similar and have a shallow positive slope (black and red

curves). In the third night the spectrum was almost flat (green curve).

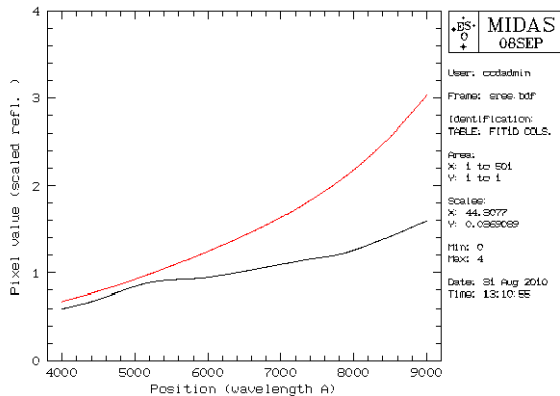


Figure 9: Spectra of faint (~16 mag), high AMR ($0.5 \text{ m}^2/\text{kg}$), ‘eccentric GEO’ debris E07046Bn taken on different nights.

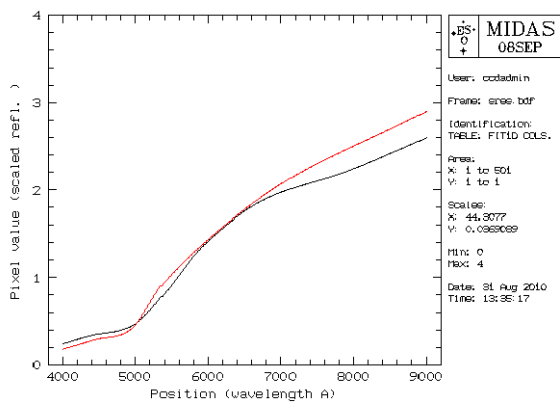


Figure 10: Spectra of faint (~16 mag), high AMR ($3.0 \text{ m}^2/\text{kg}$), ‘eccentric GEO’ debris object N2010067 measured on different nights.

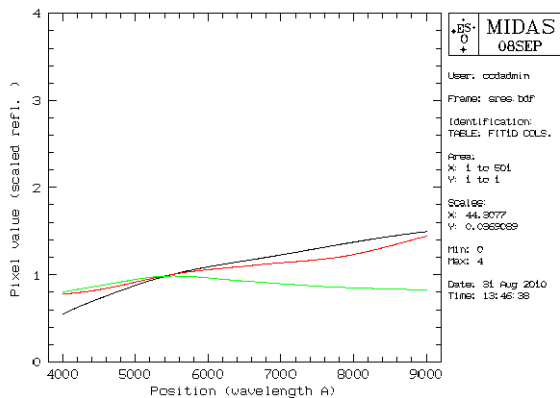


Figure 11: Spectra of faint (16.3 ± 0.8 mag), high AMR ($29.3 \text{ m}^2/\text{kg}$), ‘eccentric GEO’ debris object S95300 measured on different nights.

Comparison with laboratory spectra

Several solar cell and Multi-Layer Insulation (MLI) samples were measured at the AIUB facility in Zimmerwald with an Oceanoptics USB2000+ spectrometer. The samples included different types of solar cells, among them solar cells retrieved from the Hubble Space Telescope (HST), as well as ‘gold’ Kapton and ‘silver’ MLI.

Some of the object spectra show substantial similarity with the spectra obtained in the laboratory. Figure 12 shows the spectrum of the object N2010067 (already presented in Figure 10) and the Kapton MLI spectrum measured in the laboratory. Both spectra exhibit a sharp bend around 500 nm. After 600 nm the reflectance data start to diverge, the values for the space object increasing much faster. This difference in the slope could be due to the ‘reddening effect’.

A second example is shown in Figure 13 where a measurement of object S95300 (see also Figure 11) is compared with laboratory measured values of a ‘silver’ MLI sample. Both spectra are a very flat curve with some differences only at the blue end for wavelength shorter than 500 nm. The fact that the object S95300 has a very high AMR may justify the hypothesis that this debris object is a piece of MLI material, known to be very light and thin.

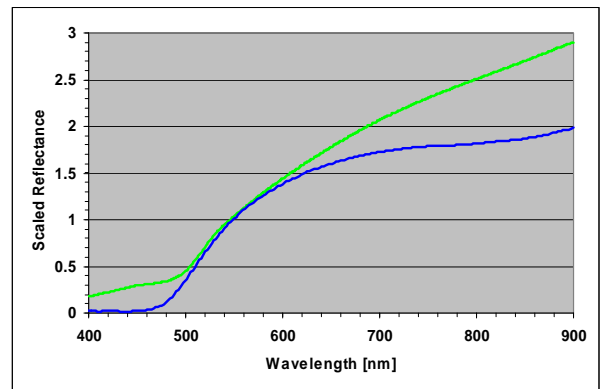


Figure 12: Spectra of object N2010067 (green; see also Figure 10) and Kapton MLI (blue).

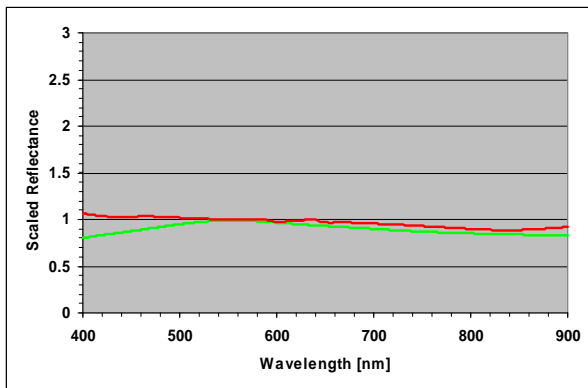


Figure 13: Spectra of object S95300 (green; see also Figure 11) and ‘silver’ MLI (red).

SUMMARY AND CONCLUSIONS

The ESA low-resolution spectrograph at the ESASDT in Tenerife was used to obtain reflection spectra of objects in high-altitude orbits. The observations had strictly experimental character and were originally aimed to obtaining spectra of bright targets only. Eventually spectra of 34 different objects in GEO, ‘eccentric GEO’ and GTO orbits were observed (4 intact spacecraft, 1 upper stage and 29 small-size debris). Among these observations there are 16 spectra of faint, high AMR debris objects in ‘eccentric GEO’ orbits.

Generally, the spectra may be grouped in three categories. The first category is characterized by a steep slope at the beginning of the infrared region with the slope increasing with increasing wavelength. Spectra in this category could be explained by the ‘reddening effect’. The second category includes spectra with an overall positive slope and a plateau in the infrared region (decreasing slope with increasing wavelength). A third group contains spectra with a negative slope at the blue end, a relatively flat region between 600 nm and 800 nm and a positive slope in the infrared region.

A subset of the measured objects shows different spectra for different measurement epochs. For some objects two different spectra were observed repeatedly, which indicates that likely two different faces of the same rotating or tumbling object were measured.

The so-called ‘reddening effect’ experienced by materials exposed to the space environment is poorly understood, difficult to model, and thus severely limits the comparison of the remotely ob-

served spectra with laboratory spectra of spacecraft materials. For a handful of the high AMR objects the observed spectra match laboratory spectra of single materials. In particular the spectrum of a debris piece with a very high AMR of $29.3 \text{ m}^2/\text{kg}$ is consistent with laboratory spectra of ‘silver’ MLI and for a debris object with $\text{AMR}=3.0 \text{ m}^2/\text{kg}$ a good match with Kapton (‘gold’) MLI was found.

ACKNOWLEDGMENTS

The ESA observations were acquired under ESA/ESOC contracts 21447/08/F/MOS. The HST solar cell sample was provided by G. Drolshagen (ESTEC), the triple-junction solar cell sample by F. Piergentili (La Sapienza), and the multi-layer insulation material data by K. Abercromby. The collaboration with the Keldysh Institute of Applied Mathematics (KIAM) and the ISON was instrumental in maintaining the orbits of the targeted debris objects. The authors would like to thank J. Kuusela and D. Abreu for mounting the spectrograph and taking the observations.

REFERENCES

- [1] Schildknecht, T., R. Musci, T. Flohrer, Properties of the High Area-to-Mass Ratio Space Debris Population at High Altitudes, 36th COSPAR Scientific Assembly, July 16-23, Beijing, China, 2006, Advances in Space Research, Vol. 41, pp 1039–1045.
- [2] Schildknecht, T., R. Musci, C. Früh, M. Ploner, Color Photometry and Light Curve Observations of Space Debris in GEO, 2008 AMOS Technical Conference, pp 496–501, 16-19 September, Maui, Hawaii, USA, 2008.
- [3] Seitzer, P., K J. Abercromby; H. M. Rodriguez-Cowardin, E. Barker; G. Foreman, M. Horstman, Photometric Studies of Orbital Debris at GEO, 5th European Conference on Space Debris, March 30 – April 2, ESOC, Darmstadt, Germany, 2009.
- [4] Jorgensen, K., J. Africano, K. Hamada, P. Sydney, E. Stansbery, P., Kervin, D. Nishimoto, J. Okaba, T. Thumm, K. Jarvis, Using AMOS Telescope for low Resolution Spectroscopy to Determine the Material Type of LEO and GEO Objects, 2001 AMOS Technical Conference, pp 127–134, 10-14 September, Maui, Hawaii, USA, 2001.
- [5] Jorgensen, K., Okada, J., Guyote, M., Africano, J., Hall, D., Hamada, K., Barker, E., Stansbery, G., Kervin, P., Reflectance Spectra of Human-Made Objects, 2004 AMOS Technical Conference, Maui, Hawaii, USA, 2004.
- [6] Abercromby, K., Guyote, M., Okada, J., Barker, E., Applying space weathering models to common spacecraft materials to predict spectral signatures, 2005 AMOS Technical Conference, Maui, Hawaii, USA, 2005.